Brain Perfusion SPECT in Alzheimer's Disease

11

Kiyotaka Nemoto

Abstract

Over the last decade, research using positron emission tomography (PET) or single photon-emission computed tomography (SPECT) has revealed the distinguishing regional cerebral hypometabolism or hypoperfusion in various neurodegenerative disorders, which is useful for differential diagnosis of diseases. In addition to that, development of statistical analysis of neuroimaging data unveiled the subtle changes which was difficult to notice with visual inspection. SPECT findings of typical AD are characterized with hypoperfusion in (1) parietotemporal association cortex, (2) posterior cingulate gyrus and precuneus, and (3) medial temporal areas. Hypoperfusion in these regions might be a predictor for cognitive decline. With these findings, the neuroimaging examinations have become essential in clinical settings for the purpose of diagnosis of very early Alzheimer's disease (AD) at a prodromal stage, prediction of conversion from mild cognitive impairment (MCI) to AD, or differential diagnosis from other diseases causing dementia.

Keywords

Alzheimer's disease • SPECT • Precuneus • Parietal cortex • Hippocampus

K. Nemoto
Department of Neuropsychiatry, Institute of Clinical Medicine, University of Tsukuba, 1-1-1 Tennodai, Tsukuba, Ibaraki 305-8575, Japan
e-mail: kiyotaka@nemotos.net

H. Matsuda et al. (eds.), *Neuroimaging Diagnosis for Alzheimer's Disease and Other Dementias*, DOI 10.1007/978-4-431-55133-1_11

11.1 Introduction

Over the last decade, the interest toward functional neuroimaging in the field of neurodegenerative disease has gradually increased. Research using positron emission tomography (PET) or single photon-emission computed tomography (SPECT) has revealed the distinguishing regional cerebral hypometabolism or hypoperfusion in various neurodegenerative disorders, which is useful for differential diagnosis of diseases. In addition to that, development of statistical analysis of neuroimaging data unveiled the subtle changes which was difficult to notice with visual inspection. With these findings, the neuroimaging examinations have become essential in clinical settings for the purpose of diagnosis of very early Alzheimer's disease (AD) at a prodromal stage, prediction of conversion from mild cognitive impairment (MCI) to AD, or differential diagnosis from other diseases causing dementia. In this chapter, we first review the neuropathological findings of Alzheimer's disease. Then we go through the SPECT findings of AD with basic knowledge of statistical analysis of SPECT images.

11.2 Neuropathological Legions of Alzheimer's Disease

AD is characterized by two types of lesions: amyloid deposits and neurofibrillary tangles. Amyloid deposits are the extracellular aggregation of Aβ peptide and neurofibrillary tangles composed of intraneuronal bundles of paired helical filaments which are the aggregation of pathologic tau proteins. Both lesions extend progressively to neocortical brain areas during the course of AD. Braak and Braak [1] found that initial changes occur in the transentorhinal region and extend to entorhinal region, Ammon's horn, and neocortex. Delacourte and colleagues [2] further categorized the disease progression in ten stages: transentorhinal cortex, entorhinal, hippocampus, anterior temporal cortex, inferior temporal cortex, medium temporal cortex, polymodal association areas, unimodal areas, primary motor or sensory regions, and all neocortical areas. They also found that the disease could be asymptomatic unless polymodal association areas are affected and that individuals with two polymodal association areas affected by tau pathology showed cognitive impairment. In summary, degeneration occurs initially in limbic regions and extends to neocortices. Clinical symptoms become apparent after the legions affect polymodal association areas.

11.3 Principle of Statistical Mapping

Due to the low spatial resolution, it is not easy to detect subtle hypoperfusion of SPECT images with visual inspection, which results in low intra- and inter-rater reliability [3]. Statistical analysis approach is a way to visualize the hypoperfusion regions plain and clearly. An example is shown in Fig. 11.1. The subject is a

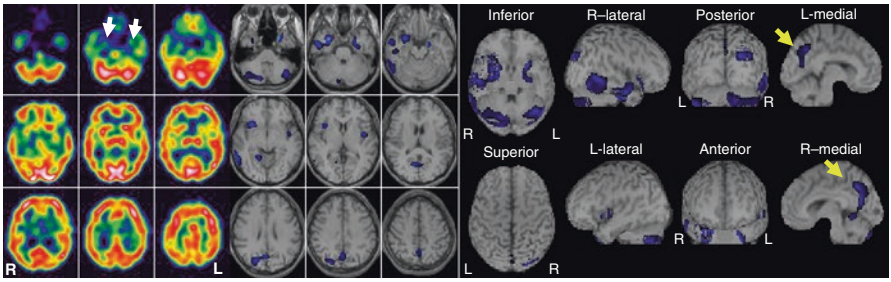

Fig. 11.1 An example of the result of statistical analysis of SPECT image. It is not easy to point out the hypoperfusion regions with visual inspection of SPECT image except for hypoperfusion in medial temporal regions. However, statistical analysis with easy z-score imaging software (eZIS) reveals hypoperfusion in precuneus in addition to hippocampal hypoperfusion. These results are quite persuasive and easy to understand for not only medical staffs but also patients and their families

76-year-old male. One may notice hypoperfusion in bilateral medial temporal regions (arrows in white), but other areas look quite normal with visual inspection. However, statistical analysis reveals hypoperfusion in bilateral precunei (arrow in yellow) in addition to medial temporal regions. These results are quite persuasive and easy to understand for not only medical staffs but also patients and their families. Two software packages are widely used in clinical settings in Japan. One is easy Z-score imaging system (eZIS) developed by Matsuda et al. [4] and the other is three-dimensional stereotactic surface projection (3D-SSP) developed by Minoshima and colleagues [5]. Since both software packages take similar process, here we see the process of eZIS. Note that eZIS employs statistical parametric mapping software (SPM) for normalizing and smoothing of the images.

11.3.1 Preprocessing (Normalizing and Smoothing)

Each individual has a different size and shape of the brain. In order to compare data from several subjects, all the images need to be in the same space. In eZIS which employs SPM, this is accomplished by "normalizing" the images into the space defined by the Montreal Neurological Institute (MNI) template. The detail of normalizing process is described by Ashburner, one of the developers of SPM [6].

Following spatial normalization, the image data would be "smoothed" or blurred. By smoothing, the signal-to-noise ratio is increased. It also ensures that the residual differences are closer to Gaussian and decreases the intersubject registration error. Another reason for smoothing is simplifying the ensuing results, producing fewer regions of significant difference to report [7]. The outline of preprocessing is illustrated in Fig. 11.2.

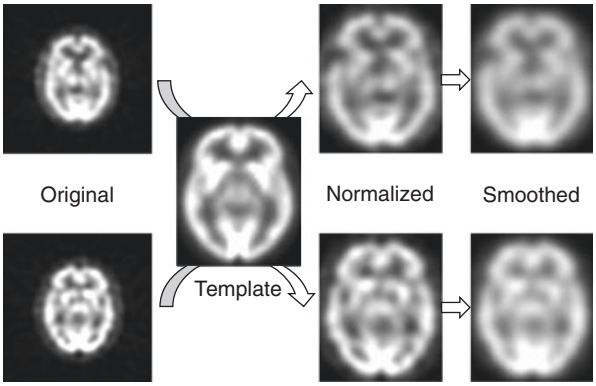

Fig. 11.2 A scheme of preprocessing. In order to compare data from several subjects, data are normalized to the space defined by the Montreal Neurological Institute template. Following spatial normalization, the image data are smoothed to be suited for statistical analysis

11.3.2 Generating Z-Score Images

After preprocessing, intensity of each image is normalized. Note that eZIS takes a different approach from SPM. In SPM, intensity normalization takes a two-step procedure. First, it calculates mean of an image. This averages all of the voxel values (VV) even outside the brain, so we need to threshold the image with certain value. Threshold is calculated by mean divided by 8. Then it calculates global value by averaging the VV above the threshold. Finally global value is set to 50 mL/min/100 g and each VV is adjusted with proportional scaling.

On the other hand, eZIS takes a straightforward procedure. First it applies a brain mask to preprocessed images. Then mean value is calculated with the masked images. Setting global value and adjusting VV is the same as SPM. Figure 11.3 illustrates how mean and VV of a certain voxel will change throughout the procedure. VV of a voxel coordinate [40 30 40] in the preprocessed image is 796.0 and mean VV is 368.8. Note that at this point, mean includes voxels outside the brain. After masking, VV at [40 30 40] remains the same, but the mean changes from 368.8 to 635.1. Now using proportional scaling eZIS sets mean as 50, VV at [40 30 40] will be $796.0 \times \frac{50}{635.1} = 62.7.$ Understanding this procedure is important because sometimes we see apparent hyperperfusion regions in eZIS results. For example, global cerebral blood flow (CBF) of advanced demented patients is generally low such as 30 mL/min/100 g, but the regional CBF in primary sensory motor region is intact such as 45 mL/min/100 g. In this case, after intensity normalization, the adjusted regional CBF in primary somatosensory regions will be $45 \times \frac{50}{30} = 75,$

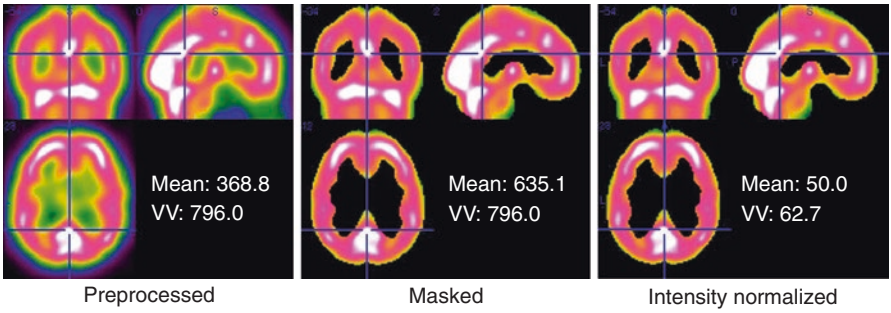

Fig. 11.3 Illustration of how mean and voxel values (VV) of a certain voxel will change by masking and proportional scaling

which will result in remarkable hyperperfusion in this region. In order to prevent misinterpreting the results, it is recommended to check the global CBF regularly.

Following intensity normalization, z-score at each voxel is calculated with the following equation.

$$\text{Z score} = \frac{\text{average of control VV} - \text{subject VV}}{\text{SD of control VV}}$$

Here SD stands for standard deviation. This equation can be rephrased like the following.

$$\text{Subject VV} = \text{average of control VV} - \text{Z score} \times \text{SD of control VV}$$

So if Z-score is 2, one can say that subject's VV in a certain voxel is 2 standard deviation below average of control subjects. This equation also tells us that we need to prepare the mean and standard deviation of control subjects beforehand. Z-score highly depends on the quality of control subjects, so we need to keep in mind that using different control subjects might result in quite a different result.

Z-score images are overlaid on the standard brain as shown in Fig. 11.1. Z-score threshold is an arbitrary set. In Fig. 11.1, z-score = 2 is set as a threshold.

11.4 SPECT Findings in Alzheimer's Disease

SPECT findings of typical AD are characterized by hypoperfusion in (1) the parietotemporal association cortex, (2) posterior cingulate gyrus and precuneus; and (3) medial temporal areas [8]. It is also noteworthy that CBF of primary sensorimotor region is spared until the advanced stage. The yellow arrows in Fig. 11.4 point the characteristic hypoperfusion regions in AD and red arrow points the primary sensorimotor region where CBF is spared.

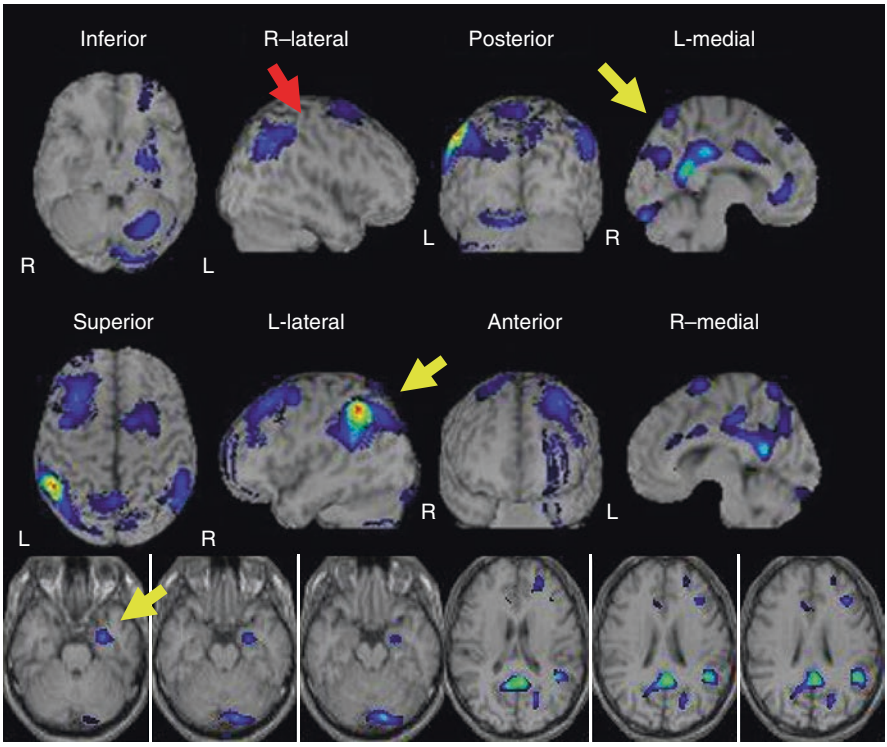

Fig. 11.4 SPECT findings of typical AD are characterized by hypoperfusion in the (1) parietotemporal association cortex, (2) posterior cingulate gyrus and precuneus, and (3) medial temporal areas. Note that CBF of the primary sensorimotor region is spared until the advanced stage. The *yellow arrows* point the characteristic hypoperfusion regions in AD, and the *red arrow* points the primary sensorimotor region where CBF is spared

11.4.1 Parietotemporal Cortex

The parietotemporal cortex is the first cortical region to be affected in AD [8]. Kemp and colleagues reported that early-onset AD patients have greater posterior association cortex involvement than those with late onset [9]. Hypoperfusion regions extend to the frontal lobes except for primary sensorimotor region as the disease progresses.

11.4.2 Posterior Cingulate Gyrus and Precuneus

Hypoperfusion or hypometabolism in the posterior cingulate gyrus (PCG) and precuneus is the very early finding of AD. Indeed, even patients with amnestic MCI patients show hypoperfusion in the region [10]. Though statistical image analysis clearly demonstrates the hypoperfusion in PCG and precuneus, one can notice the

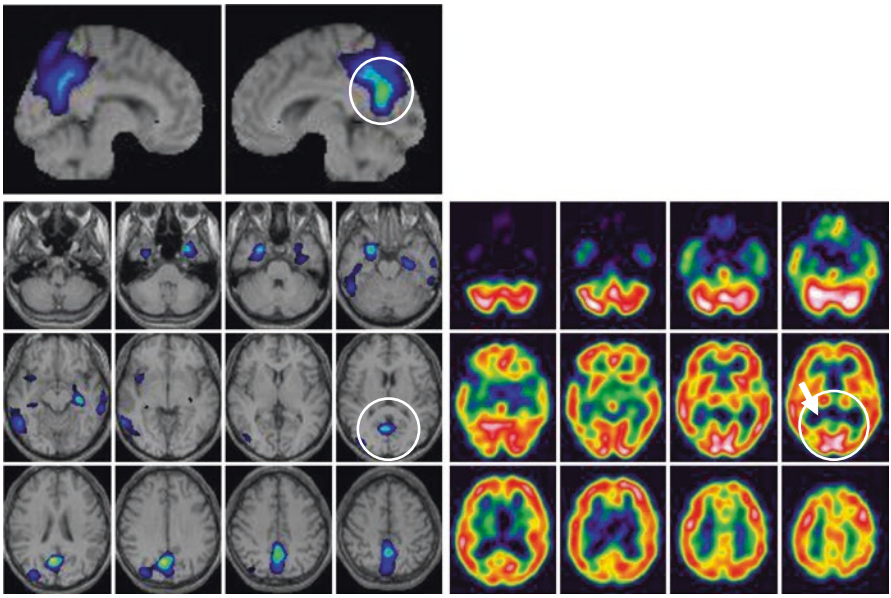

Fig. 11.5 A key to notice hypoperfusion in PCG and precuneus. The *white circle* shows the hypoperfusion in PCG and precuneus. Note the dip in SPECT image shown by white arrow. This dip reflects the hypoperfusion in PCG

hypoperfusion with careful visual inspection. The white circle in Fig. 11.5 shows the hypoperfusion in PCG and precuneus. Note the dip in SPECT image shown by the white arrow. This dip reflects the hypoperfusion in PCG. Small et al. demonstrated that hypometabolism in PCG and precuneus at a presymptomatic stage predicts a future cognitive decline in people with genetic risk of Alzheimer's disease [11]. This shows that hypoperfusion or hypometabolism in PCG and precuneus is recognized well before patients show cognitive impairment.

11.4.3 Medial Temporal Areas

It is well known that AD patients show volume reduction in hippocampal regions from the very early stage [12]. SPECT images, with its lower spatial resolution, are affected by partial volume correction. This means that regional cerebral blood flow (rCBF) in hippocampal regions seems decreased despite true rCBF is not decreased. Indeed, Ishii et al. reported that rCBF at the hippocampus of mild AD patients was intact after partial volume correction [13]. Nonetheless, hypoperfusion in hippocampal regions is clinically useful because it reflects dysfunction in the hippocampus. Figure 11.6 shows hypoperfusion in the hippocampus. With axial view, temporal lobe perfusion of healthy subjects look like "crab claw" (white circle). However, it looks as if medial part of crab claw was lost when the hippocampus perfusion is reduced.

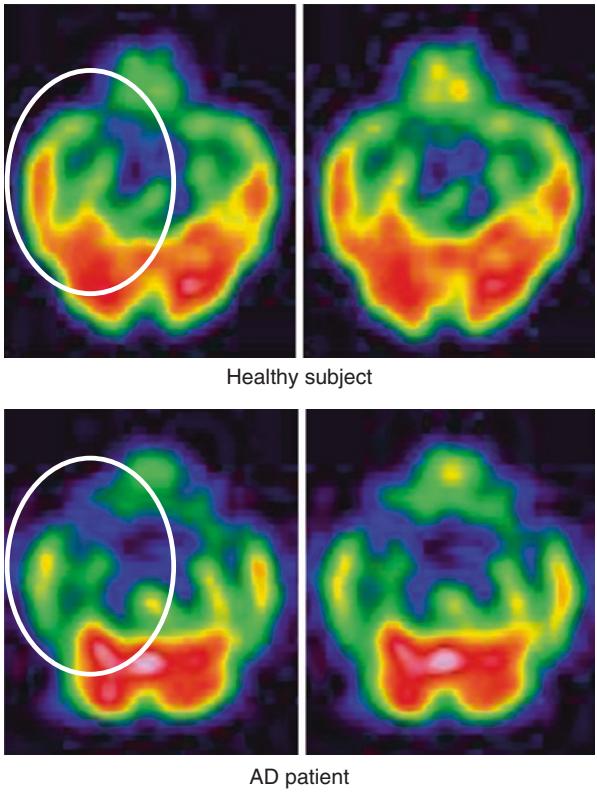

Fig. 11.6 Hypoperfusion in the hippocampus. With axial view, temporal lobe perfusion of healthy subjects looks like a "crab claw" (*white circle*). However, it looks as if the medial part of the crab claw was lost when the hippocampus perfusion is reduced

11.5 Longitudinal SPECT Changes in Alzheimer's Disease

Here we see a 71-year-old male case who was amnestic MCI at an initial visit but developed clinical AD in years. We followed up his SPECT images over 5 years (Fig. 11.7). At an initial visit, his MMSE was 26 and he complained subjective forgetfulness. At this point, SPECT showed hypoperfusion in the PCG and hippocampus. His cognition remained for 2 years. Two years after the initial visit, his MMSE was 25. However, SPECT showed progressive hypoperfusion in PCG and precuneus. From that time on, his cognition declined gradually and MMSE got 21 at 4 years from the first visit. At this time SPECT showed progressive hypoperfusion in the hippocampus. A year later his MMSE declined to 20. Note that his MMSE between initial visit and 2 years later did not change much though his rCBF showed prominent decline in PCG and precuneus. Noticing this in clinical settings is useful because it can be a predictor for cognitive decline. In this respect, just following up MMSE is not enough to predict the disease progression.

As we see in this chapter, SPECT is very useful for the diagnosis and short-term prediction of cognitive decline. If you are not sure about the diagnosis of patients with cognitive decline or want to know the perspective of patients in terms of cognitive decline, considering SPECT might be an asset.

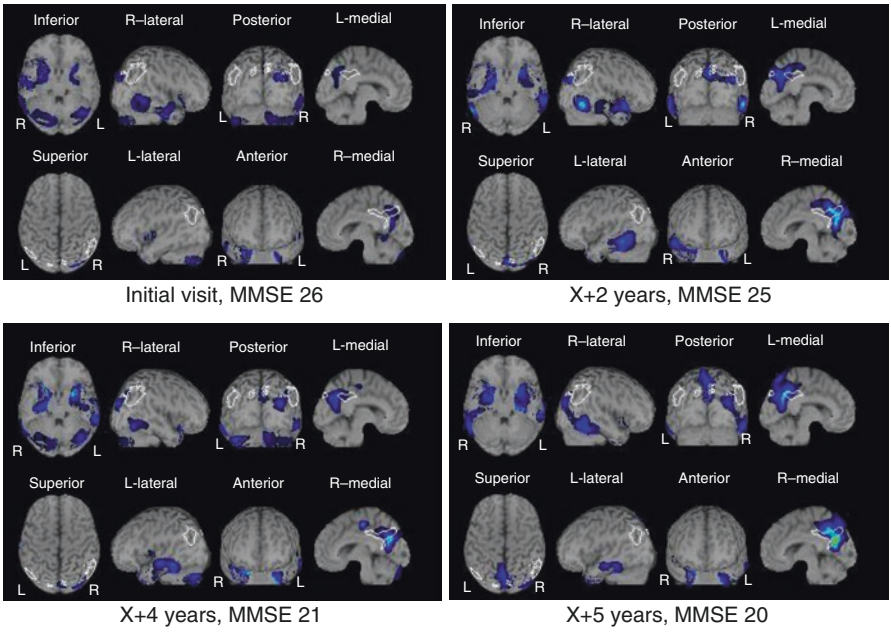

Fig. 11.7 Longitudinal rCBF change of a 71-year-old male who developed clinical AD. Note that progression of hypoperfusion in precuneus preceded the cognitive decline

References

1. Braak H, Braak E. Staging of Alzheimer's disease-related neurofibrillary changes. Neurobiol Aging. 1995;16:271–278.; discussion 278–84. doi:10.1016/0197-4580(95)00021-6.
2. Delacourte A, David JP, Sergeant N, et al. The biochemical pathway of neurofibrillary degeneration in aging and Alzheimer's disease. Neurology. 1999;52:1158–65.
3. Imabayashi E, Matsuda H, Asada T, et al. Superiority of 3-dimensional stereotactic surface projection analysis over visual inspection in discrimination of patients with very early Alzheimer's disease from controls using brain perfusion SPECT. J Nucl Med. 2004;45:1450–7.
4. Matsuda H, Mizumura S, Nagao T, et al. An easy Z-score imaging system for discrimination between very early Alzheimer's disease and controls using brain perfusion SPECT in a multicentre study. Nucl Med Commun. 2007;28:199–205. doi:10.1097/MNM.0b013e328013eb8b.
5. Minoshima S, Frey KA, Koeppe RA, et al. A diagnostic approach in Alzheimer's disease using three-dimensional stereotactic surface projections of fluorine-18-FDG PET. J Nucl Med. 1995;36:1238–48.
6. Ashburner J, Friston KJ. Nonlinear spatial normalization using basis functions. Hum Brain Mapp. 1999;7:254–66.
7. Ashburner J. Computational anatomy with the SPM software. Magn Reson Imaging. 2009;27:1163–74.
8. Kanetaka H, Matsuda H, Asada T, et al. Effects of partial volume correction on discrimination between very early Alzheimer's dementia and controls using brain perfusion SPECT. Eur J Nucl Med Mol Imaging. 2004;31:975–80. doi:10.1007/s00259-004-1491-3.
9. Kemp PM, Holmes C, Hoffmann SM, et al. Alzheimer's disease: differences in technetium-99m HMPAO SPECT scan findings between early onset and late onset dementia. J Neurol Neurosurg Psychiatry. 2003;74:715–9. doi:10.1136/jnnp.74.6.715.

10. Minoshima S, Giordani B, Berent S, et al. Metabolic reduction in the posterior cingulate cortex in very early Alzheimer's disease. Ann Neurol. 1997;42:85–94. doi:10.1002/ana.410420114.
11. Small GW, Ercoli LM, Silverman DH, et al. Cerebral metabolic and cognitive decline in persons at genetic risk for Alzheimer's disease. Proc Natl Acad Sci U S A. 2000;97:6037–42. doi:10.1073/pnas.090106797.
12. Risacher SL, Saykin AJ. Neuroimaging biomarkers of neurodegenerative diseases and dementia. Semin Neurol. 2013;33:386–416. doi:10.1055/s-0033-1359312.
13. Ishii K, Sasaki M, Yamaji S, et al. Paradoxical hippocampus perfusion in mild-to-moderate Alzheimer's disease. J Nucl Med. 1998;39:293–8.